How Bubbly Mixtures Foam and Foam Control Using a Fluidized Bed

by
José Guitián[‡]
Daniel Joseph*

August 1996, revised in Feb. 1997

[‡]Intevep S.A. VZ

*University of Minnesota
AEM, 107 Akerman Hall, 110 Union Street
Minneapolis, MN 55455

ABSTRACT

In hydrocracking and other foaming reactors, the foam rises to the top because it has a higher gas fraction than the bubbly mixture from which it comes. The high gas hold-up in foams is undesirable in chemical reactors because it strongly decreases the liquid residence time and in hydrocracking reactors also promotes the formation of coke. To study foams we built a cold slit bubble reactor which when used with aqueous anionic surfactants gives rise to foam. This reactor reproduces the foaming processes which are characteristic of the commercial system CANMET from Petrocanada. We discovered a critical condition for foaming; when the gas velocity exceeds a critical value which depends on the liquid velocity, a foam interface appears at the top of the reactor, with foam above and bubbly mixture below. The interface is very sharp and it moves down the reactor as the gas velocity is increased at a constant liquid velocity. This is the way reactors foam, with the bubbly mixture being consumed by foam.

The foam may be destroyed by increasing the liquid velocity backing up against the foaming threshold. The reactor partitions into two phase, two phase flow with bubbly mixture below and foam above. The bubbly mixture is dispersed gas in water plus surfactant; the phase above is a foam through which large gas bubbles rise. Constant state theories for the bubbly mixture, the foam and the position of the foam interface are derived and semiempirical correlations are presented.

Foaming may be strongly suppressed by fluidizing hydrophilic particles in the bubbly mixture below the foam. The suppression is achieved by increasing the liquid hold-up by bed expansion; by increasing the wetted area of solid surface (walls and particles) and by decreasing the gas hold-up by increasing the effective density of the liquid-solid mixture.

Industrial foaming reactors

Applications of foams and foaming are found in many industries like the flotation of minerals, enhanced oil recovery drilling in oil reservoirs, insulation, construction and refining processes such as Vacuum distillation and Delay-Coker reactors. However, foaming and defoaming are not yet well understood. The modern theory of foams could be said to start with [1973] study of Bikerman. A consolidation of the advances in the study of foams and foaming is in the collection edited by Prud'homme and Khan [1995]. Foams trap gas and are not wanted in many applications; Garrett [1993] has edited a collection of papers on defoaming. Our application area is to unwanted foaming in foaming bubble reactors and the practical application of our study is the suppression of foaming. To achieve this goal we propose fundamental studies of recent observations which we have made in foam suppression studies in the slit bubble reactor described in section two below.

Pruden [1993] has reported 80v% gas hold-up in the reactor of the commercial demonstration plant used in the CANMET process for a wide range of gas velocities and reactor temperatures. The overall gas hold-up values which were observed are consistent with a severe foaming condition in the reactor using a typical commercial gas velocity. In the CANMET process, foam formation was detected in the commercial unit only because of the higher gas velocities employed. Under typical hydrocracking conditions using catalytic slurry reactors of the bubble column type and catalysts, foam may be present in the reaction zone. Foaming can occur at temperatures higher than 400°C which are typical in industrial reactors.

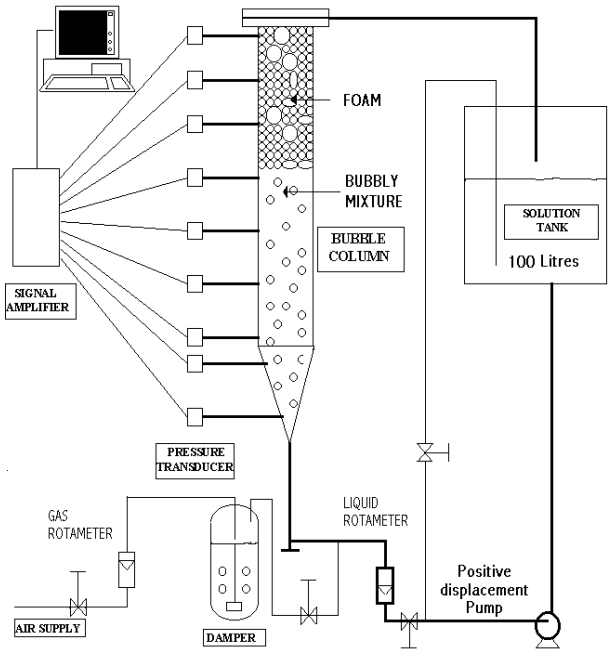

Figure 1: Diagram of the bubble column: height 170 cm, width 26 cm and depth 1.3 cm. Flow lines are clearly visible through the thin Plexiglas column. The metal screen at the top of the column which is used to hold solid particles in the reactor does not have a major effect on the flow below.

Slit bubble reactor.

To evaluate the fluid dynamics of a foaming bubble column with a continuous gas/liquid input, we constructed apparatus shown in Figure 1. Nine highly accurate pressure transducers were installed. The output of each pressure transducer is in the mV range and is amplified to the 0-10V range. This signal is fed into a PC, where the signal is converted to pressure and a time average is constructed. The total and local average gas hold-up in the column is calculated using the pressure obtained at different times. Measurements were taken at a rate of 30 per second for a period of 3 minutes after reaching a stable state. The time required for transients to decay depends on the operating conditions and the foaming capacity of the surfactant mixtures. Steady states are recognized in foaming systems by the stabilization in the pressure values in the column and by visual observation of the foam interface. The time required to reach steady state was between 30 min. and 60 min. depending basically on the liquid and gas velocities.

The superficial gas velocity U_g and liquid velocity U_l are prescribed data which we control in our bubble column. Figure 1 shows the experimental equipment in the foaming mode. The total average gas fraction $\epsilon_g = 1 - V_l/V$ in steady flow was determined by direct measurement of the liquid volume V_l after the gas and liquid flows were stopped simultaneously and by a second method based on the pressure drop (ΔP_t) which is the sum of the static pressure drop (ΔP_s) and the pressure drop due to friction between two points separated by a distance (ΔH). However, at gas and liquid velocities normally employed in bubble columns, the pressure drop due to the friction is relatively small and the local gas fraction between the two points is given by

$$\epsilon_g = 1 - \frac{\Delta P_s}{g\rho_l \Delta H} \qquad (1)$$

The two methods agree when $\Delta H = L$ showing that the pressure drop due to friction is negligible. The variation of the total gas fraction with gas velocity, using foaming systems, in the laboratory reactor in Figure 1 is in astonishing agreement with published data for the CANMET reactor (see Figure 6).

Part 1: Foam formation at an interface

When the superficial velocity of the gas exceeds a critical value which depends on the foaming properties of the liquid and its superficial velocity, a foam/bubbly mixture interface appears at the top of the reactor as shown in Figures 1 and 3. The interface is very sharp and it moves down the reactor as the gas velocity is increased at a constant liquid velocity. This is the way the reactor foams, with the bubbly mixture being consumed by foam. You can eliminate foam entirely by increasing the liquid velocity beyond a threshold set by the gas velocity.

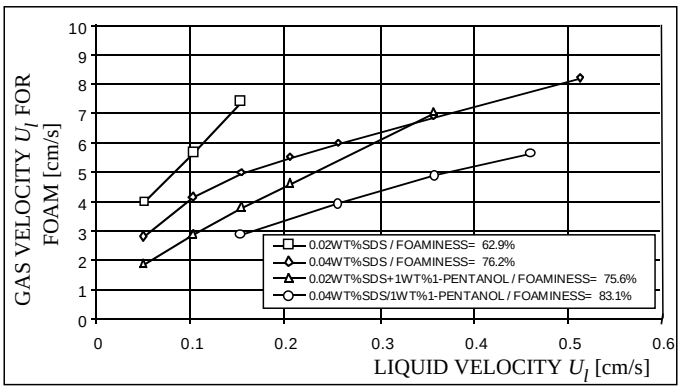

Figure 2: Plots of equation (2) giving U_g and U_l for the inception of foaming. The constants a and b in (2) depend on the properties of the surfactant solution.

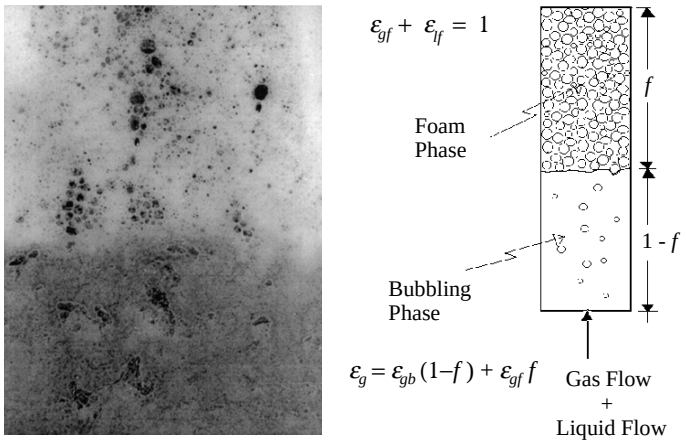

Figure 3: Foam regions in two phase foaming systems. $f = h/H$, where H is the total height of the reactor and h is the height of the foam.

The interface defines a change of phase of a *two-phase, two-phase flow;* the bubbly mixture is a two phase flow of gas and surfactant in water; the foam is also two phase flow of gas and surfactant in water but is better characterized as a foam though which large gas bubbles rise. When characterized in this way, gas bubbles are always the dispersed phase; surfactant in water is the continuous phase in the bubbly mixture and the foam is continuous in the foamy mixture. The interface marks a phase change for the continuous phase from surfactant in water to foam.

The reader should maintain distinction between the foam which is a structure of fluid with films and plateau borders and foamy mixture in which large gas bubbles rise though the foam. However, in the sequel we shall not always call attention to this distinction between foam and foam though which large gas bubbles rise.

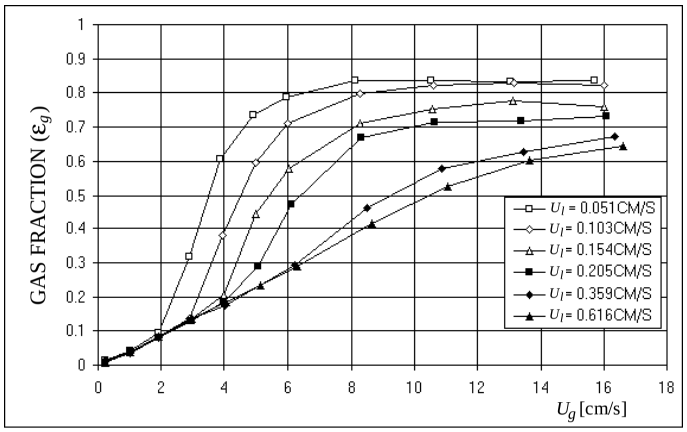

Figure 4: Gas fraction as a function of gas velocity: Water/0.02wt%SDS/1 wt% 1-Pentanol.

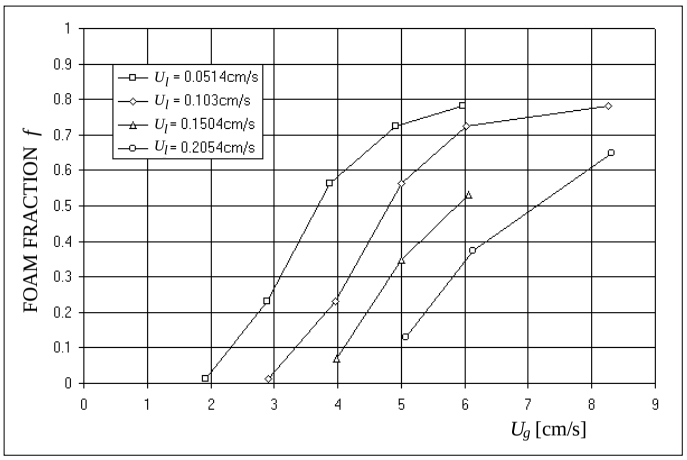

Figure 5: Foam fraction f as a function of gas velocity: Water/0.02wt%SDS/1 wt% 1-Pentanol.

Critical condition for the appearance of foam.

The critical condition for the appearance of foam can be approximated by the equation

$$U_g = a + bU_l \tag{2}$$

where U_g and U_l are superficial velocities and a and b empirical constants independent of these velocities (see Figure 2). If U_g is less than U_g in (2) for a given U_l, there will be no foam in the reactor; the reactor will be filled to the top with bubbly mixture. When U_g reaches the critical value in (2), foam appears at the top of the reactor. The foam is separated from the bubbly mixture by a sharp interface (see Figure 3); as U_g is increased past the critical value, more and more of the bubbly mixture is consumed by foam.

Figure 4 shows some typical results giving the total gas fraction in the reactor as a function of the superficial gas velocity U_g for different liquid velocities U_l. Foaming does not occur in pure liquids without surfactants. Foaming also does not occur in foaming liquids when the liquid velocity is larger than the threshold value defined by (2). The bottom curve in Figure 4 is for a non-foaming high liquid flow situation. Foaming begins when U_g goes critical. This occurs for smaller values of U_g when U_l is low, at values where the upward sloping branches bifurcate from the non-foaming branch. Consistent with (2) is the fact that there is more gas for a given U_g when U_l decreases. The maximum gas fraction for this foam is slightly above 80% which can be considered a typical value.

The increase in the total gas fraction in the reactor due to foaming is shown in Figure 4; the foam height $f = h/H$ is also an increasing function of U_g as shown in Figure 5.

Figure 6 shows the comparison between the laboratory reactor with foaming systems and the results of the commercial demonstration reactor of the CANMET process (Pruden [1993]), owned by Petrocanada, for the hydroconversion of heavy crudes using bubble column reactors. The cold laboratory reactor reproduces the gas fraction behavior as a function of gas velocity of such commercial unit. Fan et al. [1987] have noted the gas hold-up in coal liquifaction reactors can be simulated using pentanol/water systems.

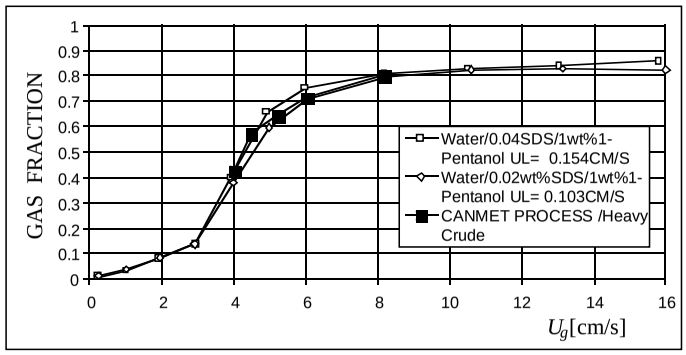

Figure 6: Comparison between gas fraction in CANMET process and cold model experimental results (Figure 1) using Water/SDS/1-Pentanol Systems. The CANMET hydrocracking reactor is 2 meters in diameter with a capacity of 800Ton/day and operates at a temperature greater than 400°C.

Constant state theory

The simplest possible theory arises from assuming that the bubbly mixture and the foam are in constant states, with constant gas fraction (ϵ_{gb} in the bubbly mixture and ϵ_{gf} in the foam). The superficial velocities are related to the gas fractions by Richardson/Zaki type correlations which are completed by linear regression from reactor data.

Following Wallis [1969] we express the slip velocity in terms of the gas fraction ϵ_g by

$$\nu_g - \nu_l = \frac{U_g}{\epsilon_g} - \frac{U_l}{(1-\epsilon_g)} = U_{b\infty}\Phi(\epsilon_g) \tag{3}$$

where $U_{b\infty}$ is the terminal velocity of a single bubble and $\Phi(\epsilon_g)$ depends only on ϵ_g.

The terminal velocity of a spherical bubble which rises freely as a hard sphere in a liquid/surfactant has been calculated by Matsumoto and Morooka [1989] and is given by

$$\frac{U_{b\infty} D_b \rho_l}{\mu_l} = \frac{Ga}{\left[18^{4/5} + (Ga/3)^{2/5}\right]^{5/4}} \tag{4}$$

where Ga is the Galilei number $(D_l^3 \rho_l (\rho_l - \rho_g) g/\mu_l^2)$. Linear regression of our data using (4) gives $\Phi(\epsilon_g)(1-\epsilon_g) = 1$. Hence the fraction in the bubbly mixture can be explicitly obtained from (3) as

$$\epsilon_{gb} = \frac{U_g}{U_g + U_l + \left[\dfrac{\mu_l Ga}{D_b \rho_l \left[18^{4/5} + (Ga/3)^{2/5}\right]^{5/4}}\right]} \tag{5}$$

The computation of the bubble size D_b in a bubble column is rather complicated and is described in the appendix.

To predict the gas fraction in the foam we use (3) again written as

$$\frac{\nu_g}{\nu_l} = \frac{U_g}{\epsilon_{gf}} \frac{(1-\epsilon_{gf})}{U_l} = \frac{U_{b\infty}\Phi(\epsilon_{gf})(1-\epsilon_{gf})}{U_l} + 1 \tag{6}$$

In the limiting case of very dry foams, the gas is trapped in the foam; the water and gas move in lock step on $\nu_g/\nu_l = 1$; the term $U_{b\infty}\Phi(\epsilon_{gf})(1-\epsilon_{gf})/U_l$ in equation (6) is equal to zero. Regression analysis of our data shows that $U_{b\infty}\Phi(\epsilon_{gf})(1-\epsilon_{gf})/U_l$ is constant for all foams. This is a surprising result which implies that equation (6) can be simplified to

$$\frac{U_g}{\epsilon_{gf}} \frac{(1-\epsilon_{gf})}{U_l} = \frac{\nu_g}{\nu_l} = \Omega \tag{7}$$

The two equations (7) may be solved for

$$U_g = \frac{U_l \epsilon_{gf}}{1-\epsilon_{gf}} \Omega \tag{7}_1$$

where

$$\epsilon_{gf} = 1 - \frac{U_l(\Omega - 1)}{\nu_g - \nu_l} \tag{7}_2$$

showing that ϵ_{gf} and then U_g are determined by the slip velocity $\nu_g = \nu_l$ in the foam and the superficial velocity U_l. We may also replace U_g in (5) with $(7)_1$; this shows that ϵ_{gb} also is determined by $\nu_g - \nu_l$ and U_l.

The constant Ω in this equation should be a function of the foaminess of each foaming system. Some typical values of Ω are (7.4, 7.6, 6.5) for aqueous (0.04wt%SDS, 0.04wt%SDS/1wt%1-Pentanol, 0.02wt%SDS/1wt%1-Pentanol) solutions. Relaxing our assumption of constant states for the moment, we note that the gas in the foam is partitioned into a fast moving part which rises through the foam and a trapped part which moves with the foam. Neglecting drainage, the foam velocity $\nu_f = \nu_l$. Then ν_g is apparently associated with fast rising large gas bubbles since $\nu_g = \Omega \nu_l$ and the slip velocity $\nu_g - \nu_l$. may then also be regarded as the difference between the velocity of fast rising gas bubbles through the foam and the foam itself.

Phase change Interface

The two constant states are greatly different; the gas fraction ϵ_g is much larger and the gas velocity $\nu_g = U_g/\epsilon_g$ is much smaller in the foam than in the bubbly mixture. We find it remarkable that these two constant states are separated by a sharp interface shown in Figure 3 at the critical condition (2) and moves down the column as U_g increases. We do not pretend to understand the physics which gives rise to this interface and we have only an ad hoc theory to predict its position.

The existence of two constant states with greatly different gas fractions separated by a sharp interface occurs in counterflow bubble reactors and has been analyzed using a drift flux theory (Wallis [1969]). This theory gives rise to two solutions for the gas fraction corresponding to observations with systems that are not able to produce foam, but does not predict the position of the interface.

The physics of a counterflow bubble reactor with rising bubbles and falling liquid is very different than foaming reactors because surfactants are not involved and the discontinuity in the gas fraction does not involve a change of phase at a boundary separating two two-phase flows (bubbly mixture and foam). This latter transition involves morphological transformation analogous to phase change in crystalline solids. Another way to think of the phase change from bubbly mixture to foam is in analogy to evaporation with an equilibrium "temperature" U_g and "pressure" U_l satisfying a vapor-liquid like phase change equation (2).

We could say that the system allows two solutions, one without foam, and the foaming solution which has a lower energy.

To predict f, we looked at the mechanical energy dissipation, following Gidaspow's [1994] treatment of transient one dimensional particulate flow. In the constant state theory, all derivatives except dp/dx are put to zero. Since we found in experiments that at the operating conditions normally used in bubble columns, (moderate values U_g and U_l), the pressure drop is balanced by the static pressure head, we can neglect the gas wall friction and liquid wall friction. Therefore, the liquid momentum balance is given by

$$-(1-\epsilon_g)\frac{dp}{dx} - (1-\epsilon_g)\rho_l g + \beta(\nu_g - \nu_l) = 0 \tag{8}$$

and the gas momentum balance by

$$-\epsilon_g \frac{dp}{dx} - \epsilon_g \rho_g g - \beta(\nu_g - \nu_l) = 0 \tag{9}$$

after eliminating dp/dx, we get

$$g(\rho_l - \rho_g) = \frac{\beta(\nu_g - \nu_l)}{\epsilon_g(1-\epsilon_g)}. \tag{10}$$

The friction factor parameter β can be related to the drag coefficient by the balance of buoyancy and drag

$$\frac{4}{3}\pi\Big(\frac{d_b}{2}\Big)^3 g(\rho_l - \rho_g) = \pi\Big(\frac{d_b}{2}\Big)^2 \frac{1}{2}\rho_l(\nu_g - \nu_l)^2 C_D \tag{11}$$

where C_D is the drag coefficient. From (10) and (11) we find that

$$\beta = \frac{3}{4}\frac{\rho_l \epsilon_g(1-\epsilon_g)C_D(\nu_g - \nu_l)}{d_b} \tag{12}$$

The mechanical energy equation for the gas/liquid mixture can be obtained by multiplying the liquid momentum balance (8) by ν_l and dividing by $(1-\epsilon_g)$, multiplying the gas momentum balance (9) by ν_g and dividing by ϵ_g and adding both equations. After writing

$$dp/dx = -\rho_l(1-\epsilon_g)g, \tag{13}$$

the energy equation is given by

$$\rho_l g(1-\epsilon_g)(U_g + U_l) - \rho_l g U_l - \rho_g g U_g = \beta(\nu_g - \nu_l)^2 \tag{14}$$

where $\rho_g U_g$ is much smaller than $\rho_l U_l$ and may be neglected. Equation (13) indicates that the input power to the column is dissipated by the friction associated with gas bubbles rising through the liquid.

After substituting (12) into (14) we get

$$\begin{aligned} I &= \rho_l g(1-\epsilon_g)(U_g + U_l) - \rho_l g U_l - \rho_g g U_g \\ &= \tfrac{3}{4}\tfrac{\rho_l \epsilon_g(1-\epsilon_g)C_D(\nu_g-\nu_l)^3}{d_b} = D \end{aligned} \tag{15}$$

Equation (15) relates the power input per unit volume of column (I) on the left to the power dissipated per unit volume of column due to the friction between the phases (D) on the right. An expression for the bubble size in a foam has been determined by Haas [1967] using different type of surfactants

$$d_b^2 = \alpha\frac{U_g}{(1-\epsilon_{gf})} \tag{16}$$

where α is a constant function only of the foaming system employed.

To determine α it is necessary to obtain additional information. We did visual measurements of the bubble size of the foam using high speed filming in two different foaming systems and we found that the foam bubble size is between 2mm and 4mm when 6cm/s $< U_g <$ 11cm/s and 0.05cm/s $< U_l <$ 0.15cm/s. This gives rise to the average α values given in Table 1.

When surfactants are present and foam appears we shall assume that the ratio of foam fraction to bubbly mixture

System	Gas Velocity [cm/s]	Liquid Velocity [cm/s]	Average Foam Bubble Diameter [cm]	Average α from equation (16) [cm/s]
Water/ 0.04wt% SDS	4.9	0.05	0.2	9×10^{-4}
	8.1	0.05	0.3	
	6.0	0.1	0.3	
	8.2	0.1	0.3	
	10.5	0.1	0.4	
Water/ 0.04wt%SDS/ 1wt%1-C5	4.9	0.154	0.2	20×10^{-4}
	6.0	0.154	0.2	
	8.2	0.154	0.3	

Table 1: Bubble size and constant a from equation (16).

fraction is equal to its power dissipation ratio in each of the phases; in other words

$$\begin{aligned} \frac{f}{1-f} &= \frac{D_f f}{(I_b(1-f) + I_f f) - D_f f} \\ &= \frac{\textit{Energy dissipated in foam}}{\textit{Energy dissipated in bubbly mixture}} \end{aligned} \tag{17}$$

where I_b is the power input per unit volume of the bubble phase I_f the power input per unit volume of foam (LHS of equation 15), D_f the power dissipated per unit volume of foam (RHS of equation 15). Equation (15) implies that the power dissipated per unit volume of foam and the power dissipated per unit volume of bubbly mixture are equal. We don't propose (17) as a correct statement of physics; it is an ad hoc assumption which is true for $f = 0$ and $f = 1$ and appears not to wander far from the truth for $0 < f < 1$. After substituting (15) into (17) we find that

$$f = \frac{\frac{3C_D\epsilon_{gf}(1-\epsilon_{gf})}{4gd_b}\Big(\frac{U_g}{\epsilon_{gf}} - \frac{U_l}{1-\epsilon_{gf}}\Big)^3 - \big((1-\epsilon_{gb})(U_g+U_l) - U_l\big)}{(1-\epsilon_{gf})(U_g+U_l) - (1-\epsilon_{gb})(U_g+U_l)} \tag{18}$$

where, following the discussion of (7), slip velocity in the foam

$$\nu_g - \nu_l = \frac{U_g}{\epsilon_{gf}} - \frac{U_l}{(1-\epsilon_{gf})} \tag{19}$$

may also be regarded as the difference in the velocity of the large gas bubbles which rise through the foam and the foam itself. Equations (7) show that f/C_D is a function of $\nu_g - \nu_l, U_l$ and material parameters.

The drag coefficient for a solid sphere moving through an unbounded liquid depends on the Reynolds number (see for example Dallavalle [1948], Churchill [1988]), alone and is given by empirical formulas with good accuracy. We shall assume that the same formula

$$C_D = (0.63 + 4.8Re_f^{-1/2})^2 \tag{20}$$

holds for a bubble rising through foam when

$$Re_f = \frac{(1-\epsilon_{gf})\rho_l(\nu_g - \nu_l)d_b}{\mu_f} \tag{21}$$

where μ_f is the unknown viscosity of the foam. Equations (16) and (18), together with measured values of f, determine the drag coefficient C_D; then (20) and (21) determine R_{ef} and μ_f. Equations (16)-(21) determine the foam viscosity in terms of U_l and the slip velocity, but the calculation illustrated in Figure 7 shows that μ_f is essentially independent of U_l.

Princen and Kiss [1989] derived an expression for the foam viscosity depends on the slip velocity and ϵ_{gf}. If we use the foam of their analytic expression for μ_f and fit their constants and exponents by nonlinear regression using our data for water /0.04% SDS we get

$$\mu_f = \frac{0.8177\epsilon_{gf}^{0.76}}{d_b\dot{\gamma}} + \frac{60.08(\epsilon_{gf} - 0.69)}{[d_b\dot{\gamma}]^{2.96}} \tag{22}$$

with a regression coefficient of $R^2 = 0.98$. Equation (22) can be compared with a similar equation in the abstract of the paper by Princen & Kiss [1989]. In their formula $d_b\dot{\gamma} = \nu_g - \nu_l$ but ϵ_{gf} is assumed to be given and is not computed from dynamics.

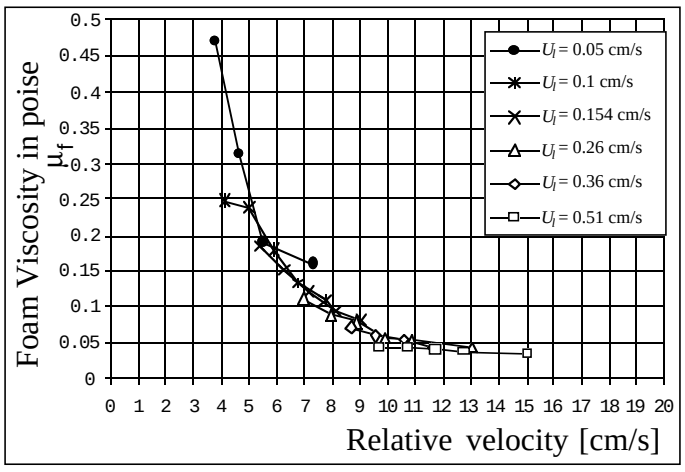

Figure 7: Foam viscosity as determined by equation (21). The derivation of this equation shows that in principle the foam viscosity depends on flow variable $\nu_g - \nu_l$ and U_l, but this figure shows that μ_f can be well approximated by a function of the slip velocity alone; regression of the data gives $\mu_f = 8.0(\nu_g - \nu_l)^{-2.151}$ with a regression coefficient $R^2 = 0.9893$.

Part 2. Foam control using a fluidized bed

1. Fluidization of particles in the bubbly mixture

Particles in batch may be fluidized in the bubbly mixture, but not in the foam. Since the particles are loaded in batch, the initial solids fraction $\epsilon_p = \frac{4n\pi}{3}a^3/V$, where n is the number of particles, a is the radius and V is the volume of the reactor, does not change once the solids are loaded into the reactor. The volume fractions (or hold-ups) of liquid ϵ_l and gas ϵ_g are also fractions relative to V, but these continuous variables depend on input velocities U_l and U_g.

Since no particles or a very small number of particles enter the foam, the effective concentration of particles is the ratio $\frac{4}{3}\pi a^3 n$ of solids to V_s which is the volume in the bubbly mixture occupied by the slurry (see figure 10).

2. Foam rheology and the foam barrier

The foam is an elastic network of films and plateau borders which maintains a locked grid structure as it moves slowly and uniformly through the bed. Large gas bubbles rise rapidly through the foam, but the foam itself does not circulate as an ordinary fluid and particles which are driven into the foam are either trapped there or fall out, but they do not circulate. The trapped particles show that the foam has a yield stress; the slow motion of the locked grid shows that the foam yields at the walls and the flow can be associated with a viscosity and the fact that particles which fall out of the foam draft, kiss and *chain* as in a viscoelastic fluid (figure 1) rather than draft, kiss and tumble as in a Newtonian fluid shows that the falling particles see a viscoelastic fluid (see Joseph et al. [1994] and [1996]).

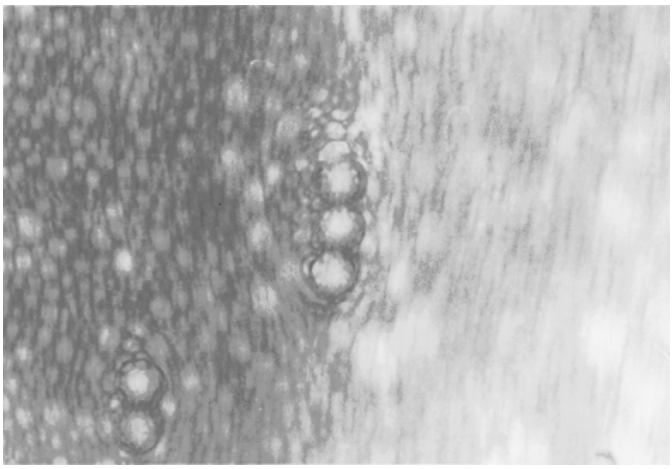

Figure 8: Particles falling in the foam tend to chain as in viscoelastic fluid.

The criterion (1) for foaming is not strongly affected by the presence of particles; the mixture will foam when the gas velocity is high enough even in a fixed bed. The foam at top of the reactor acts as a barrier to further expansion of particles in the fluidized bed and the creation of more foam by increasing the gas input compresses the fluidized bed.

3. Foam suppression with glass and plastic spheres

Prior literature (Garret [1993], Bikerman [1973], Prud'homme & Khan [1996]) on the use of particles to destroy foam describe effects of hydrophobic particles which attack the foam. Fluidization of hydrophilic particles to increase the liquid fraction (hold-up) under a foam barrier has not been discussed before.

We found that we could suppress foam by fluidizing hydrophobic particles in the bubbly mixture. This suppression can be framed as a decrease in the gas fraction or an increase in the liquid fraction of the bubbly mixture. Such effects have been reported for gas bubbles rising in pure liquids which dont foam but the decrease in the gas fraction in the pure liquid case is at best 20% compared to the 75% reduction which can be achieved in foaming systems.

For a simple mixture the gas fraction in the reactor is a linear combination of the gas fraction in each region.

$$\epsilon_g = \epsilon_{gf} f + (h - f)\epsilon_{gb} + \epsilon_{gs}(1 - h) \tag{23}$$

where $f = X_f/H$, $h = X_p/H$, ϵ_{gb} is given by (5), ϵ_{gf} is given by (7) and we propose that

$$\epsilon_{gs} = \epsilon_{go}\Phi + \epsilon_{gb}(1 - \Phi) \tag{24}$$

where ϵ_{go} is the gas fraction in the packed bed formed from all the particles in the slurry and $\Phi = C_s/C_o$ is the ratio of the volume concentration of spheres $C_s = \frac{4}{3}\pi n a^3/V_s$ in the expanded slurry to the concentration $C_o = \frac{4}{3}\pi n a^2/V_o$ in the packed bed. Here V_s is the volume of the fully expanded slurry under foam (figures 9 and 10) and V_o is the volume of the packed bed. When $C_s = C_o, \epsilon_{gs} = \epsilon_{go}$; when C_s tends to zero for a very expanded bed, $\epsilon_{gs} \to \epsilon_{gb}$. There is at present no theory giving the volume fraction C_s of fluidized spheres fully expanded under a foam barrier. A typical case giving the foam fraction f as a function of U_g for a fixed U_l is shown in figure 9 and in the explanatory cartoon shown in figure 10. Most of the data points in the figures below are for the fully expanded case $h = f$.

The control variables entering into the description of the effects on foam height of fluidizing spheres of one size are the size, density and initial solids fraction of spheres ϵ_p which is determined once and for all by the number of spheres which are loaded into and remain in the reactor. We have already noted that the effective concentration C_s of spheres in a fully expanded bed under the foam is determined by the dynamics of the bed and cannot be given a-priori. At first, the solids

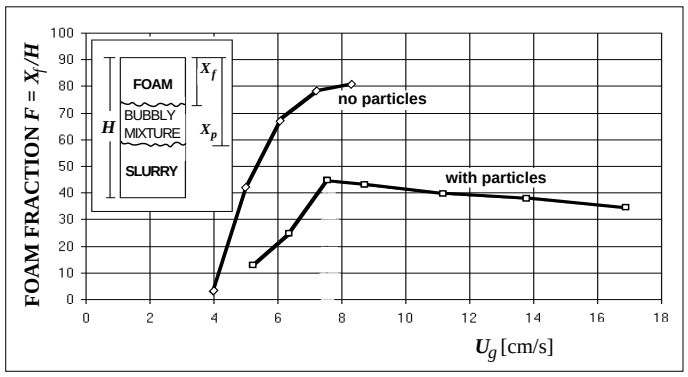

Figure 9: Effect of 532μm glass particles on foam formation in a reactor of height H with $U_l = 0.257$cm/s. The fluidized particles in the slurry suppress the formation of foam even when the slurry is not expanded, $X_f < X_p$. For $U_g > U_g^*(\approx 7.5\text{cm/s})$, the bed is fully expanded $X_f = X_p$ and its further expansion for increasing U_g appears to be inhibited by the foam.

in bubbly mixture expand in the usual way independent of the initial solids fraction. As the gas velocity is increased the bed expands more and the foam barrier falls until they touch. Then the bed is fully expanded under foam.

In section 5 we shall show that the gas fraction ϵ_g in a foaming reactor is decreased when (1) the initial solids fraction ϵ_p of particles of fixed size and density is increased (figures 11 & 12), (2) the size of particles at fixed ϵ_p and density is decreased (figures 13 & 14)and (3) the density of particles of fixed size and concentration is decreased. To explain these trends we need first to discuss the mechanisms of foam suppression.

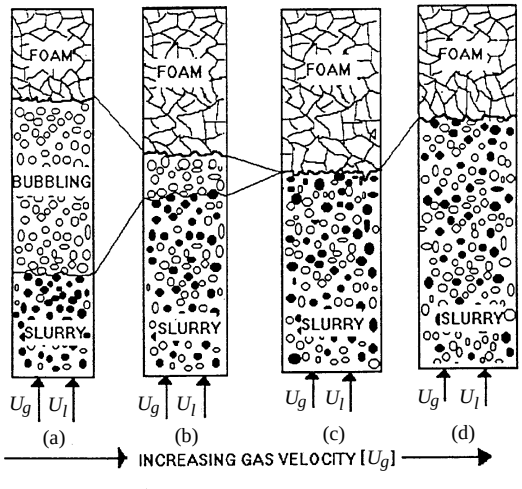

Figure 10: Particles in the bubbly mixture suppress foam even when they are not fully expanded as in (a) and (b). In (c) and (d) the fluidized bed and foam both expand against each other as the gas velocity is increased (cf. figure 9).

4. Mechanisms of foam suppression

The suppression of foam may be explained as an increase in the liquid hold-up in bubbly mixture by fluidized particles or by a decrease in gas hold-up. These effects are associated with increases in (1) the effective density of the liquid-solid mixture, (2) the area of effective wetted walls and (3) bed expansion. Gas bubbles rise faster in the composite liquid because the effective buoyant lift is greater, decreasing gas hold-up. This effect occurs both in foaming and non-foaming bubble columns.

Hydrophilic particles suspended in a bubbly mixture increase the effective area of walls wetted by liquid. Fluidized particles are stationary in an average sense so that liquid on the wall is held back. Another way to say this is that the average forward velocity of liquid is reduced by no-slip relative to an effective stationary wall composed of the reactor walls plus the wetted surface of fluidized particles.

The expansion of a bed of particles without a foam barrier should not depend on the initial batch loading ϵ_p. However, the foam barrier prevents the further expansion of a fully expanded bed in the bubbly mixture under the foam trap (see figure 9). The effective concentration of such an expanded bed does depend on the batch loading and V_s, thus C_s is a monotonic function of ϵ_p; the effective concentration increases with the batch loading.

The bed expansion is the third and possibly most important mechanism of foam suppression. The more that we can expand a bed of hydrophilic particles, the greater will be the fraction of liquid held in the reactor. Inspection of figures 9 and 10 suggests that the sharply decreased height of foam generated for fluidizing particles struck as a balance between increasing bed expansion and increased foaming generated by increasing the gas velocity U_g at fixed liquid velocity U_l.

5. Data for foam suppression by fluidized spheres of different density concentration and size

Figures 11 and 12 show that the gas fraction decreases sharply with the initial solids fraction ϵ_p of spheres for both glass and plastic 532μm spheres, respectively; the addition of plastic or glass sharply reduces the height of the foam, or increases the height of the bubbly mixture. Comparing figures 11 and 12 for the same ϵ_p and liquid velocity shows that the gas fraction is smaller for the plastic than for the glass spheres. The lower density of plastic spheres will give rise to a greater bed expansion for particles of fixed size, concentration and fluidizing velocity.

We next consider the effects of changing the size of the particles. For spheres of the same density and initial loading ϵ_p, the smaller particles are more effective in reducing the foam (gas fraction ϵ_g) in the reactor. This effect is shown in figure 13 for plastic and in figure 14 for glass particles. We may interpret this effect as an increase in liquid hold-up

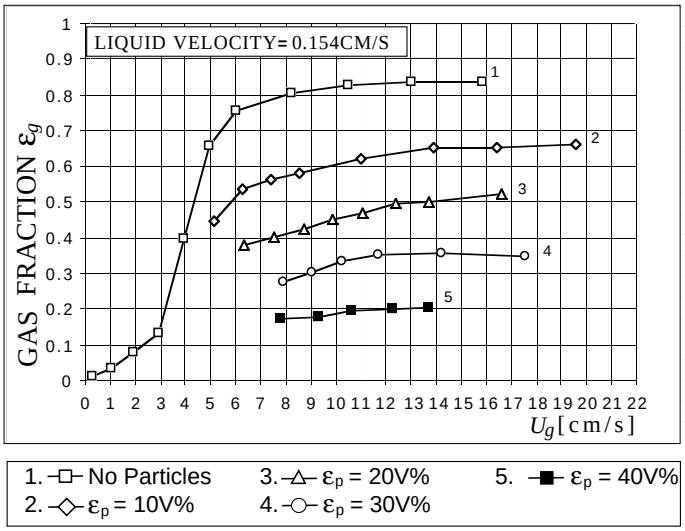

Figure 11: Gas fraction as a function of gas velocity for different initial solids fractions ϵ_p of 532 μm glass spheres.

produced by the increase in area of particles contacting liquid which you get when the size of the particles is reduced at fixed solids loading and as an increase in the bed expansion following from the reduction of the buoyant weight of small particles.

The liquid fraction for the largest 3000 μm particles is actually smaller than the liquid fraction with no particles. However, there is less foam, a smaller gas fraction ($\epsilon_g = 1 = \epsilon_l - \epsilon_p$) than in bed with no particles. Hence, the fraction ($\epsilon_l + \epsilon_p$) of liquid plus solid with large particles circulating is greater than with no particles, even though the liquid fraction is smaller (figure 15). If you need liquid in the reactor, overly large particles should not be used. Collapse of the data can be obtained by dividing $(1 - \epsilon_g)$ by the area per unit volume of reactor $6\epsilon_p/d_p$ (figure 16).

6. Summary

- A cold model bubble column reactor has been constructed in a narrow slit geometry which reproduces existing data from the literature on non foaming systems and cylindrical bubble columns. The column is equipped for high accuracy measurements of gas hold-up. The slit geometry allows us to observe the flow pattern and bubble size and to determine the presence of foam.

- The gas hold-up in non foaming systems can be correlated using the concept of slip velocity between the gas and liquid phases. The gas hold-up for water/air systems can be obtained from Richardson/Zaki type of correlations.

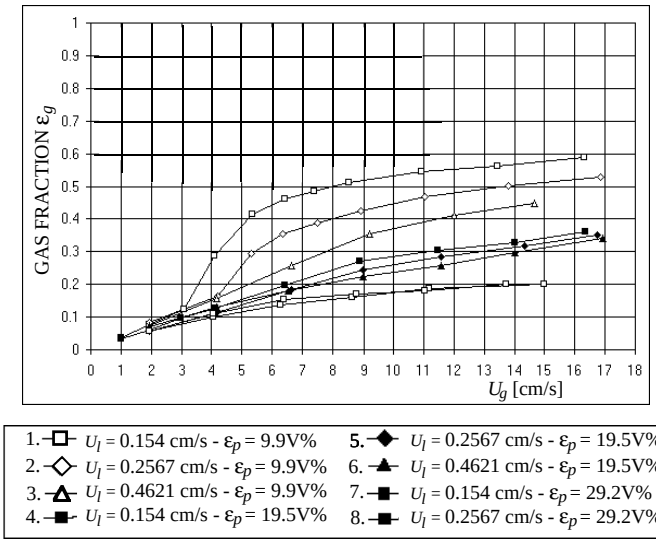

Figure 12: Gas fraction as a function of gas velocity for different initial solids fractions ϵ_p of 532 μm plastic spheres.

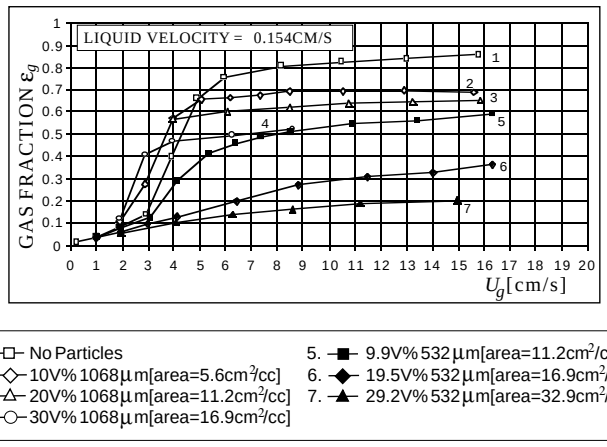

Figure 13: Effect of particle size on the gas fraction for plastic particles. The gas fraction decreases as the area of the particles increase, (size or number).

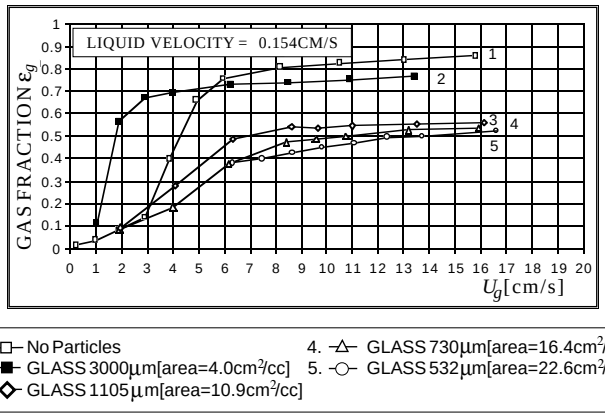

Figure 14: Effect of the particle size on the gas fraction for glass particles. The variation is monotonic in the size ($\epsilon_l + \epsilon_s = 1 - \epsilon_g$) increases with area. The largest particles have less gas but also less liquid placing a practical limitation.

- When a mixture water/surfactant is employed in the bubble column, foam can be present depending on the input parameters. Bubble and foam regimes are present at the same time in the column; the foam regime above is separated from the bubbling regime below by a very clear interface that moves down sharply when the gas velocity is increased.

- One of the most important results is that the dynamic response of the slit bubble column is nearly the same as in the large CANMET high temperature and pressure commercial reactor (2m in diameter). This result suggest that detailed studies of the characteristics of such big reactors can be obtained from relatively inexpensive slit reactors. The CANMET process can be simulated using a mixture Water/1-Pentanol/SDS.

- The total gas hold up in foaming systems can be predicted using the slip velocity concept for each of the phases (foam and bubbly mixture) by applying Richardson/Zaki type of correlations. The foam fraction is predicted by an energy balance where the ratio of the volume of foam to volume of bubbly mixture is given by the ratio of the energy dissipated in each of the phases. It is perhaps of interest that the foam height and other features of reactor respond are obtained from this energy balance in which thermodynamic correlations (temperature, interfacial energy, etc.) are totally neglected.

- The viscosity of the foam for a given foaming system is determined by the slip or relative velocity $\nu_g = \nu_l = d_b\dot{\gamma}$ and the foam gas hold up according to (22).

- Marked reduction in the gas hold-up (or foam height) of up to 75% can be achieved in a foaming reactor by fluidizing hydrophilic particles in the bubbly mixture below the foam. The gas hold-up is decreased when (1) the number of particles of fixed size and density loaded in batch (the solids loading ϵ_p) is increased, (2) the size of particles at fixed loading and density is decreased and (3) the density of particles of fixed size and loading is decreased. The decreases in gas hold-up can be associated with an increase in the buoyant lift on bubble due to an increase in the effective density of the solid-liquid mixture, the increased area of wetted walls of fluidized particles and the increases in bed expansion caused by lighter particles and reduced particle size at fixed loading.

- The fluidization of particles always increased the hold-up of solids plus liquid; if the particle size is not too large (figure 16) the liquid hold-up itself is increased by

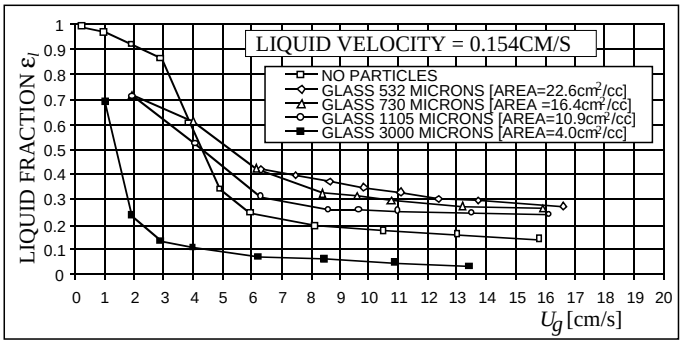

Figure 15: Effect of the particle size on the liquid fraction ϵ_l in the whole reactor. The largest particles reduce the liquid fraction below the value for no particles; however $\epsilon_l + \epsilon_g$ (3000 microns) $> \epsilon_l$ (no particles) so that the gas fraction ϵ_g is smaller. The greatest increase in the liquid fraction is produced by the smaller particles (larger area).

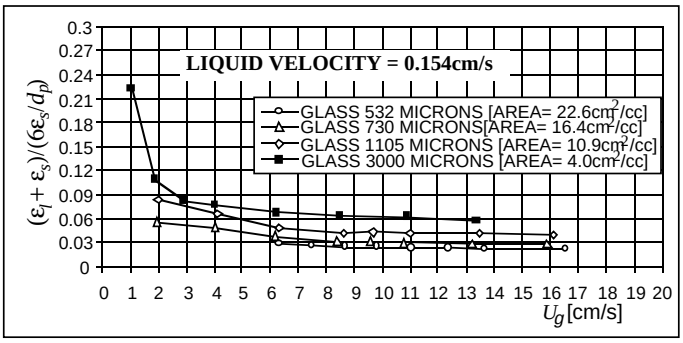

Figure 16: Ratio between $(\epsilon_l + \epsilon_g)$ and particles per unit volume of reactor as a function of gas velocity.

fluidizing particles.

- The height of foam decreases slightly in a fully expanded bed of particles under foam when the gas velocity is increased at a constant liquid velocity. This foam height is struck as balance of the tendency to increase the bed expansion by increasing the fluidizing gas velocity and to decrease the expansion by greater production of foam.

The foam barrier which keeps hydrophilic particles in a reactor and increases liquid hold-up has a certain technological potential for enhanced liquid-solid contact in commercial reactors (and forms the basis of a patent application presently under consideration).

The trends identified here should be established in greater quantitative detail. The possibility of generating increased solids hold-up in reactors with continuous rather than batch injection of particles is strongly suggested by the results given here.

Acknowledgement. This work was supported by the NSF-CTS, the office of basic energy sciences DOE, the U.S. Army (Mathematics) under DA/DAAH04-95-0106 and Intevep, S.A. A portion of the material presented here forms a part of the PhD. thesis of José Guitian in the Department of Aerospace Engineering and Mechanics (1996). We are indebted to L.S. Fan for many suggestions.

References

[1] Bikerman, J. J. (1973). *Foams*. New York: Springer-Verlag.

[2] Dallavalle, J. M. (1948). *Micrometrics*, 2nd ed. Pitman, London.

[3] Davidson, J.F. and D. Harrison (1996). The Behavior of a Continuity Bubbling Fluidized Bed. Chem. Eng. Sci., **21**, 731-738.

[4] Deckwer, W.D. (1992) *Bubble Column Reactors*. New York. Wiley.

[5] Churchill W. (1988). *Viscous Flows; The Practical Use of Theory*. Stoneham, Ma: Butterworth Publishers.

[6] Fan L. S., F. Bavarian, R. Gorowara and B. Kreischer (1989). Hydrodynamics of Gas-Liquid Fluidization under High Gas Hold up conditions. *Powder Technology*, **53**, 285-293.

[7] Garrett P. (1993) *Defoaming. Theory and Industrial Applications*. New York: Marcel Dekker, Inc

[8] Gidaspow D. (1994) *Multiphase Flow and Fluidization: Continuum and Kinetic Theory Descriptions*. New York: Academic Press.

[9] Haas, P., and H. F. Johnson (1967) A model and experimental results for drainage of solution between foam bubbles. *I & EC Fundamental*, **6**(2), 225-233.

[10] Joseph, D.D. and Feng, J. A note on the forces that move particles in a second-order fluid, *J. Non-Newtonian Fluid Mech.* **64** (1996) 299-302.

[11] Joseph, D.D., Liu, Y.J., Poletto, M. and Feng, J. Aggregation and dispersion of spheres settling in viscoelastic liquids. *J Non-Newtonian Fluid Mech.* **54** (1994) 45-86.

[12] Matsumoto T and Morooka S. (1989) Axial distribution of solid holdup in bubble column for gas-liquid systems. *AICHE Journal*, **35**(10), 1701-1709.

[13] Princen H. and Kiss A.D. (1989) Rheology of foams and highly concentrated emulsions IV., **128** (1) 176-187.

[14] Pruden B. B. (1993) The Canmet Hydrocracking Process: *Recent Developments Proceedings of the Conference Oil Sands Our Petroleum Future*, 276-282. Edmonton, Alberta, Canada.

[15] Prud'homme R and Khan S. (1995) *Foams. Theory, Measurement, and Applications.* New York: Marcel Dekker, Inc

[16] Wallis G., (1969) *One Dimensional Two Phase Flow.* New York: Mc Graw Hill.

APPENDIX

Calculation of the bubble diameter d_b in equations (4) and (5) Deckwer [1992] argued that the bubble size in a bubble column can be related to the energy density by a power law

$$D_b = k\Big[\frac{E}{V_l}\Big]^m \qquad \text{A.1}$$

where k and the exponent m are function of the system. The energy dissipation density per unit volume of liquid term E/V_l has to be evaluated in terms of the fluid dynamic parameters. In concurrent up-flow operation of bubble columns the area created and liquid re-circulation is achieved by the turbulence induced by the gas flow. Gas enters at the bottom of the column which is at a higher pressure and leaves the top at lower pressure. The pressure difference between top and bottom is given the liquid head because of pressure losses due to friction are negligible. Therefore, the amount of energy available in the column E can be obtained from the gas and liquid phase energy balance

$$E = Q_g \Delta P \qquad \text{A.2}$$

where Q_g is the total volumetric gas, ΔP is the pressure difference between the bottom and top of the column.

In a bubble column the pressure difference between the bottom and the top of the column (height H and cross section area A) can be calculated as follows:

$$\Delta P = \rho_l(1-\epsilon_g)H_g \qquad \text{A.3}$$

Substituting equation (A.1) into 3.5.18 with $Q_g = AU_g$ and dividing by the liquid volume in the column $V_l = AH(1-\epsilon_g)$, finally an expression for the power dissipation in a bubble column is obtained:

$$\frac{E}{V} = \rho_l g U_g \qquad \text{A.4}$$

Therefore, (A.1) can be written as $D_b = k(E/V_l)^m = k(\rho_l g U_g)^m$.

The fitting parameters k, m and n, in (A.1) were determined in different foaming systems by nonlinear regression. Table 2 gives the values of the fitting parameters k and m. The fitting parameter n was $n = -l$ for the three foaming systems evaluated as has been reported by Davidson et al. [1966] a regression parameter R^2 higher than 0.99, shows that a good fitting has been obtained in all the cases.

System	Fitting Parameters		Regression Parameter
	k	m	R^2
Water/0.04wt%SDS	20.255	-0.55147	0.997
Water/0.02wt%SDS 1wt	34.057	-0.6429	0.993
Water/0.04wt%SDS /1wt%1-Pentanol	38.778	-0.7148	0.997

Table 2: Fitting parameters of gas hold-up in the bubbly mixture from equation (A.1) and (5) for three foaming systems evaluated.